

## *Supporting Information*

# Steering Photoinduced Multi-Electron Accumulation via High-Concentration Sacrificial Electron Donors

*Rui Jing,<sup>1</sup> Yuhang Yang,<sup>1</sup> Junji Zhao,<sup>1</sup> Yang Li,<sup>1</sup> Di Song,<sup>\*1</sup> Hongwei Song,<sup>\*2</sup> Yan Wan,<sup>3</sup> Andong Xia,<sup>1</sup> Zhuoran Kuang,<sup>\*1</sup>*

1. State Key Laboratory of Information Photonic and Optical Communications, and School of Physical Science and Technology, Beijing University of Posts and Telecommunications (BUPT), Beijing 100876, P. R. China
2. State Key Laboratory of Luminescent Materials and Devices, Guangdong Basic Research Center of Excellence for Energy & Information Polymer Materials, South China University of Technology, Guangzhou 510640, P. R. China.
3. College of Chemistry, Beijing Normal University, Beijing 100875, P. R. China;

## AUTHOR INFORMATION

## Corresponding Author

\*Di Song E-mail: songdi@scut.edu.cn

\*Hongwei Song E-mail: songhongwei@scut.edu.cn

\*Zhuoran Kuang E-mail: kuang@bupt.edu.cn

## Contents

S1. Materials and Methods .....	3
S2. Supplementary Steady-State Absorption Spectra.....	5
S3. Supplementary Transient Absorption Spectra .....	6
S4. Reaction-Related Thermodynamic Calculations .....	12
S5. Kinetic Simulation of Multi-Electron Transfer Reactions.....	13
S6. Supplementary References .....	15

## S1. Materials and Methods

**Chemicals.** The 2,9-di(undecan-6-yl)anthra[2,1,9-def:6,5,10-d'e'f']diisoquinoline-1,3,8,10(2H,9H)-tetraone (PDI) used in this experiment was purchased from Beijing Huawei Ruike Chemical Technology Co., Ltd., and TDAE was obtained from Meryer Chemical Group. All solvents used for spectral measurement are chromatographic pure without further purification.

**Stationary Spectral Measurements.** Absorption spectra were measured on a spectrophotometer U-3900 (Hitachi, Japan), with an optical density between 0.15 and 0.3 at the peak of the lowest absorption band. Fluorescence spectra were measured on a spectrometer F-4600 (Hitachi, Japan). For fluorescence measurements, the absorbance of the solutions at the band maximum was around 0.1 OD over 1 cm.

**Femtosecond Transient Absorption Spectral Measurements.** Femtosecond time-resolved transient absorption spectra were measured using a commercial transient absorption spectrometer (Harpia-TA, Light Conversion). Briefly, fundamental pulses are derived from an amplified femtosecond Ti:sapphire laser (Astrella, Coherent). The laser delivers 40 fs pulses at 1kHz and the output is split for white-light continuum generation and optical pumping. The white-light continuum is used as a broadband optical probe from the near-UV to the visible region. It is generated by focusing the fundamental laser beam into a 2 mm thick CaF<sub>2</sub> plate, which is oriented and continuously shifted perpendicularly. The required pumping pulse is obtained by an optical parametric amplifier (TOPAS-C, Light Conversion). The pump and probe beams were overlapped on a 1 mm thick sample cell and the included polarization angle was set to the magic angle (54.7°) to record the isotropic response. The femtosecond time-resolved differential absorbance data were analyzed by using R-package TIMP software with the graphical interface Glotaran<sup>1</sup> and CarpetView (Light Conversion). UV-Vis absorption spectra of the samples are measured before and after every measurement in a spectrophotometer. No significant photodegradation was observed after the TA measurements. In the global target analysis, the differential absorbances

$\Delta A(t, \lambda)$  are decomposed as a superposition of several principal spectral components  $\varepsilon_i(\lambda)$  weighed by their concentrations  $c_i(t)$ .<sup>2</sup>

$$\Delta A(t, \lambda) = \sum_{i=1}^n c_i(t) \varepsilon_i(\lambda)$$

**Nanosecond Transient Absorption Spectral Measurements.** The ns-TA spectra were measured by a commercial spectrometer (Time-Tech Spectra). The generation of the pump beam is the same as that in fs-TA. The probe beam was generated from a supercontinuum laser (LEUKOS-DISCO, French) with the spectral region from 350 to 1800 nm, the repetition rate is 2 kHz, and pulse width is 700 ps to 1 ns. There is no photodegrading after ns-TA experiments by checking the steady-state absorption spectra.

## S2. Supplementary Steady-State Absorption Spectra

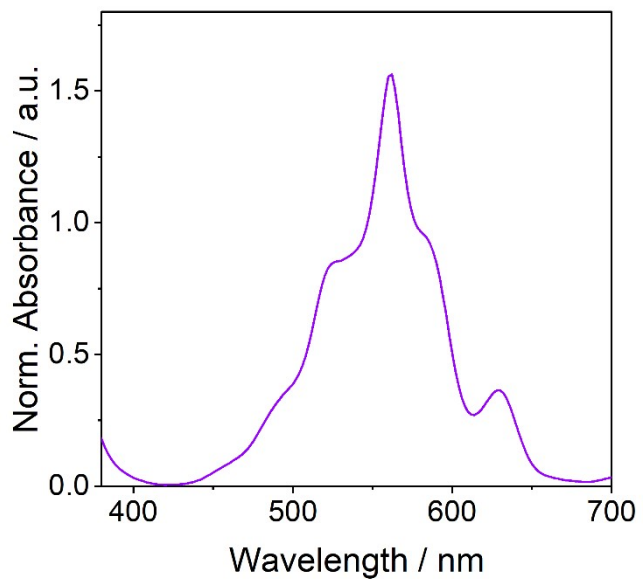


**Figure S1.** The steady-state absorption spectrum of the PDI dianion (PDI<sup>2-</sup>), obtained by chemical reduction of PDI with sodium dithionite (Na<sub>2</sub>S<sub>2</sub>O<sub>4</sub>).

### S3. Supplementary Transient Absorption Spectra

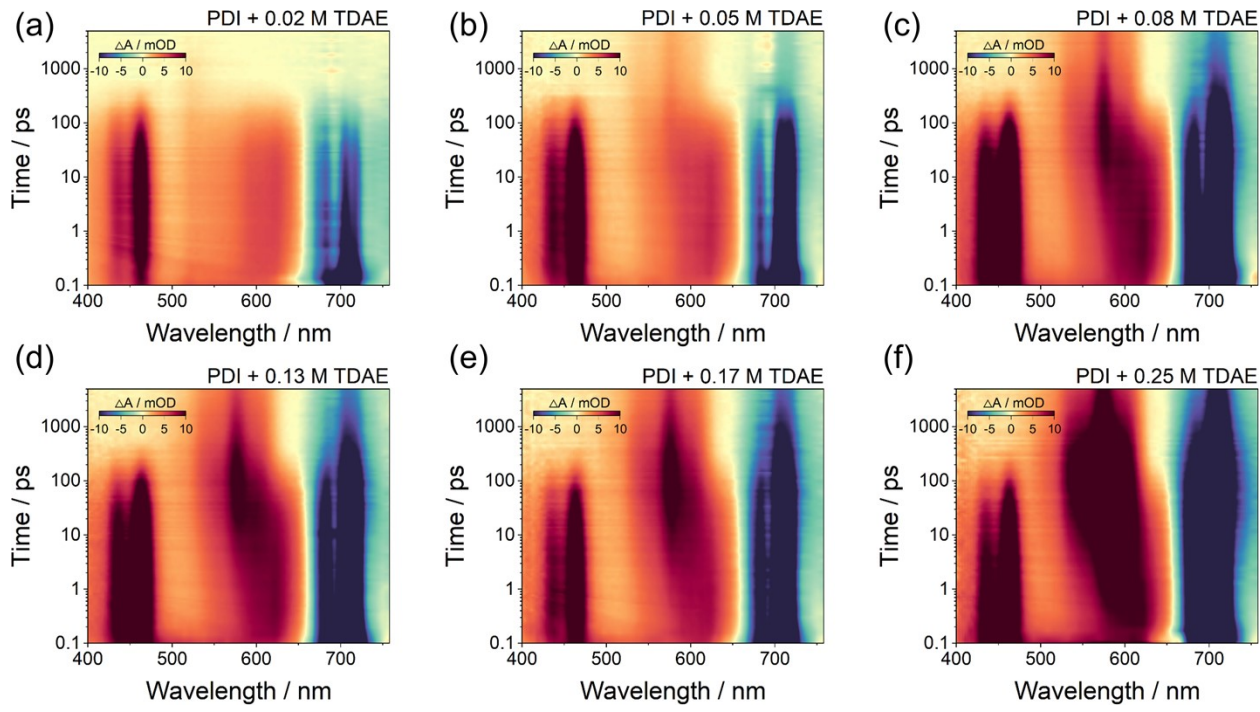


**Figure S2.** 2D-mapping fs-TA spectra of 60  $\mu\text{M}$  PDI in DMF with (a) 0.02 M, (b) 0.05 M, (c) 0.08 M, (d) 0.13 M, (e) 0.17 M, and (f) 0.25 M, TDAE upon photoexcitation at 700 nm.

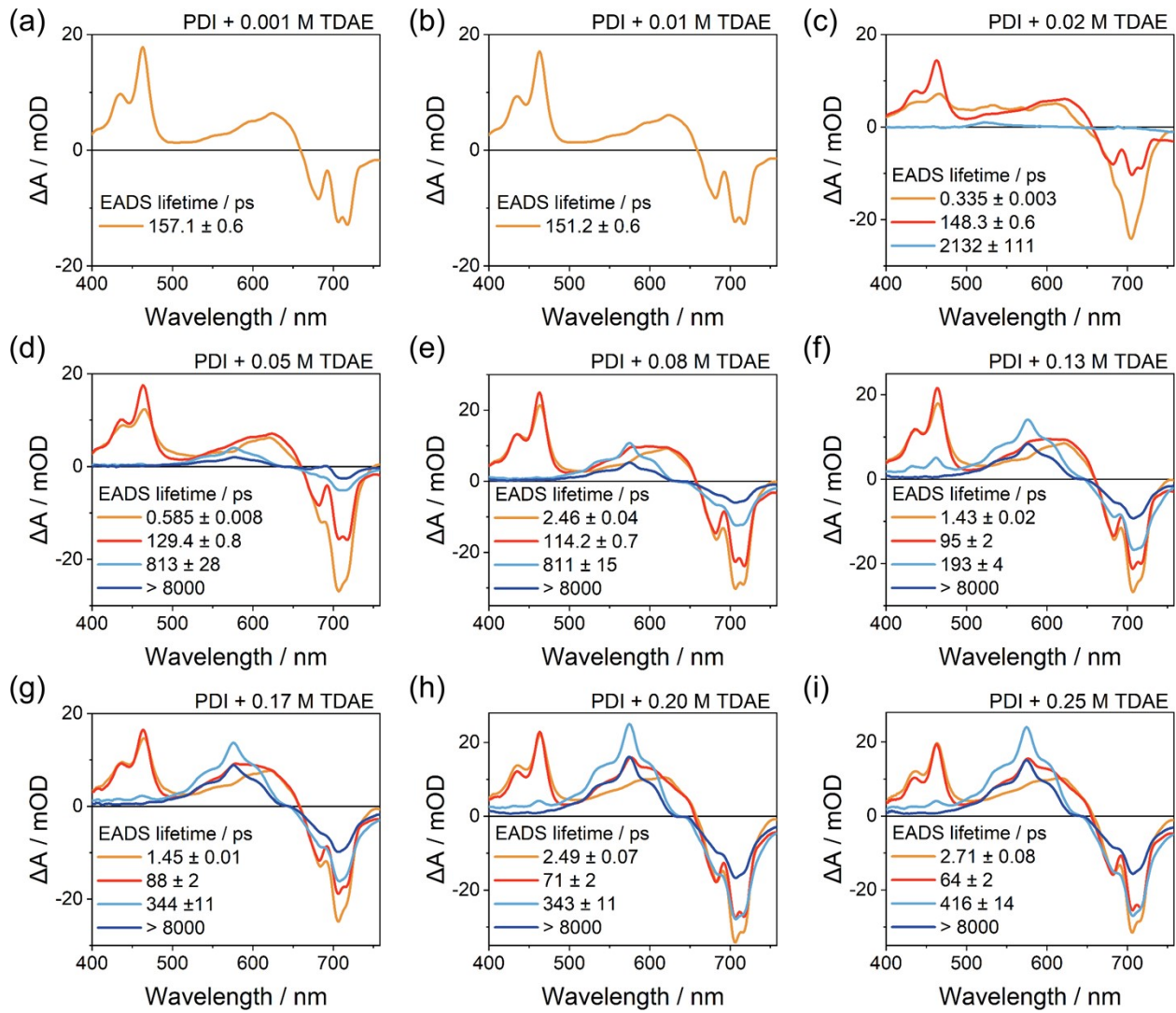


**Figure S3.** Evolution-associated different spectra (EADS) of PDI in DMF with (a) 0.001 M, (b) 0.01 M, (c) 0.02 M, (d) 0.05 M, (e) 0.08 M, (f) 0.13 M, (g) 0.17 M, (h) 0.20 M, and (i) 0.25 M TDAE obtained from the global analysis based on a sequential model. The fitting time constants are shown in legends.

**Table S1.** The lifetimes ( $\tau$ ) and corresponding quantum yields ( $\Phi$  and  $\Phi'$ ) of different concentrations of TDAE.

[TDAE] / M	$\tau$ / ps	$\Phi$ / % <sup>a</sup>	$\Phi'$ / % <sup>b</sup>
0.001	157.1	--	--
0.01	151.2	3.8	--
0.02	148.3	5.6	1.4
0.05	129.4	17.6	8.1
0.08	114.2	27.3	20.2
0.10	109.5	30.3	21.5
0.13	95	39.5	36.8
0.17	88	44.0	42.5
0.20	71	54.8	49.1
0.25	64	59.3	51.5

<sup>a</sup> The quantum yield of PDI<sup>2-</sup> derived from this excited-state lifetime-quenching method.

<sup>b</sup> The quantum yield of PDI<sup>2-</sup> determined by actinometry from the transient absorption spectra.

The PDI<sup>2-</sup> quantum yields are also determined by actinometry ( $\Phi'$ ) from the transient absorption. First, the initial concentration of photoexcited PDI<sup>•-</sup> was derived from the amplitude of the ground-state bleach signal in the evolution-associated difference spectra (EADS) obtained from global analysis. The final concentration of the product, PDI<sup>2-</sup>, was then determined from the photoinduced absorption signal at the stable endpoint of the reaction kinetics. The quantum yield  $\Phi'$  is given by the ratio of the final PDI<sup>2-</sup> concentration to the initial excited-state PDI<sup>•-</sup> concentration.<sup>3</sup>

$$\Phi' = \frac{A_{PDI^{2-}} / \epsilon_{PDI^{2-}}}{A_{PDI^{\bullet-}} / \epsilon_{PDI^{\bullet-}}}$$



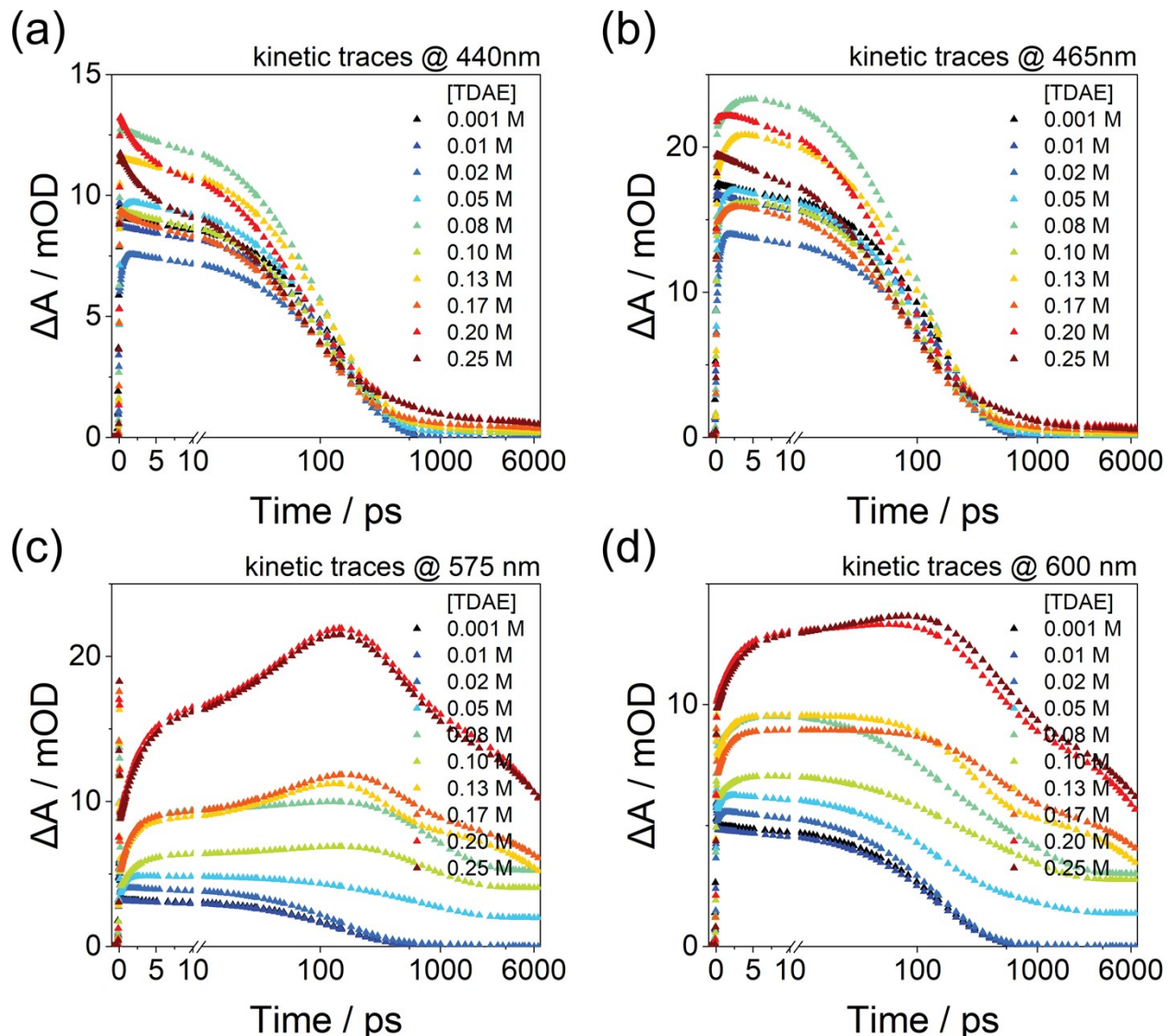


**Figure S4** The representative kinetic traces probed at (a) 440 nm (b) 465 nm (c) 575 nm and (d) 600 nm obtained from the global analysis of 60  $\mu\text{M}$  PDI in DMF with different concentration of TDAE upon photoexcitation at 700 nm.

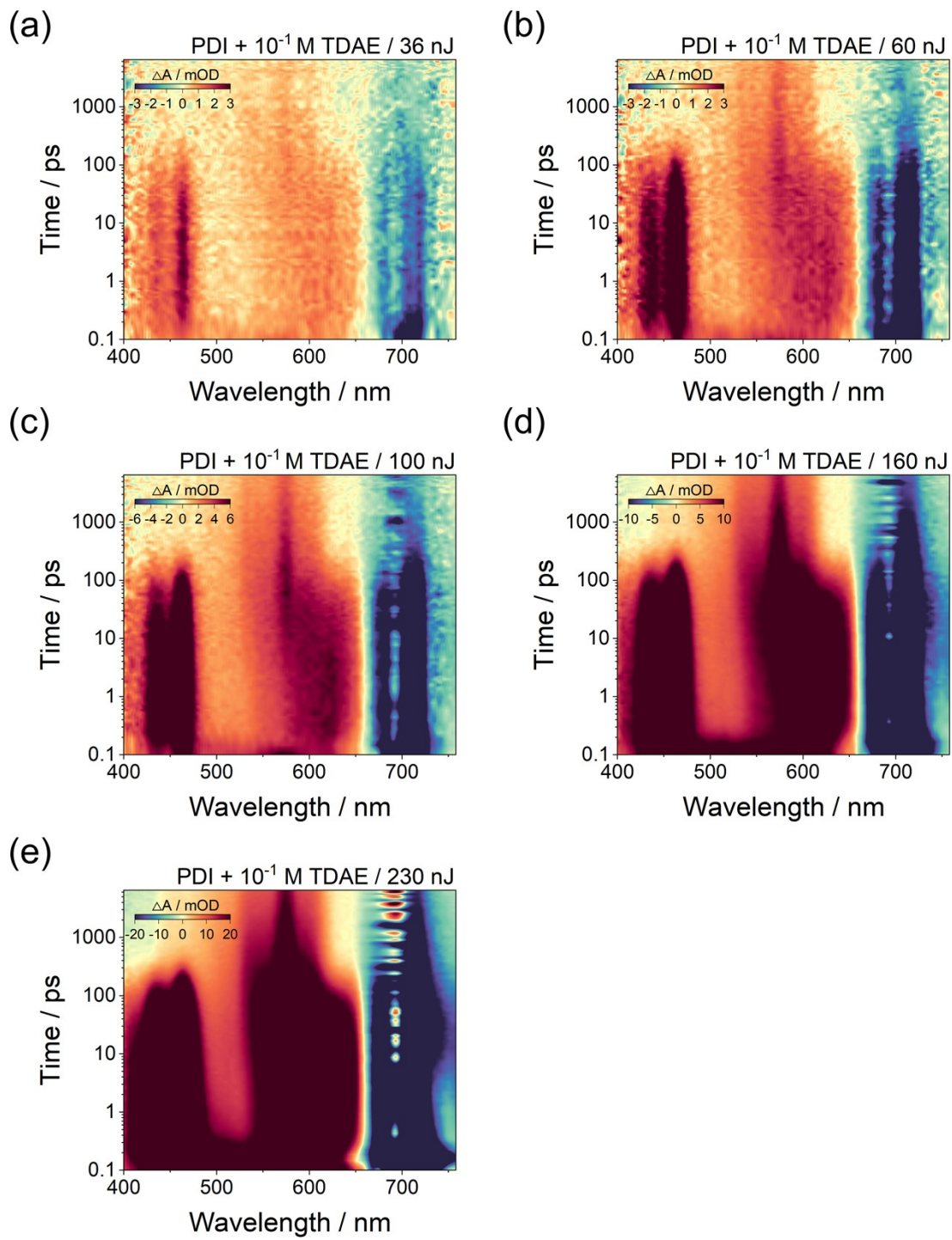


**Figure S5.** 2D-mapping TA spectra of  $60 \mu\text{M}$  PDI in DMF with  $10^{-1} \text{ M}$  TDAE upon photoexcitation under  $700 \text{ nm}$  excitation at different excitation power conditions (a)36 nJ, (b)60 nJ, (c)100 nJ, (d)160 nJ, and (e)230 nJ.

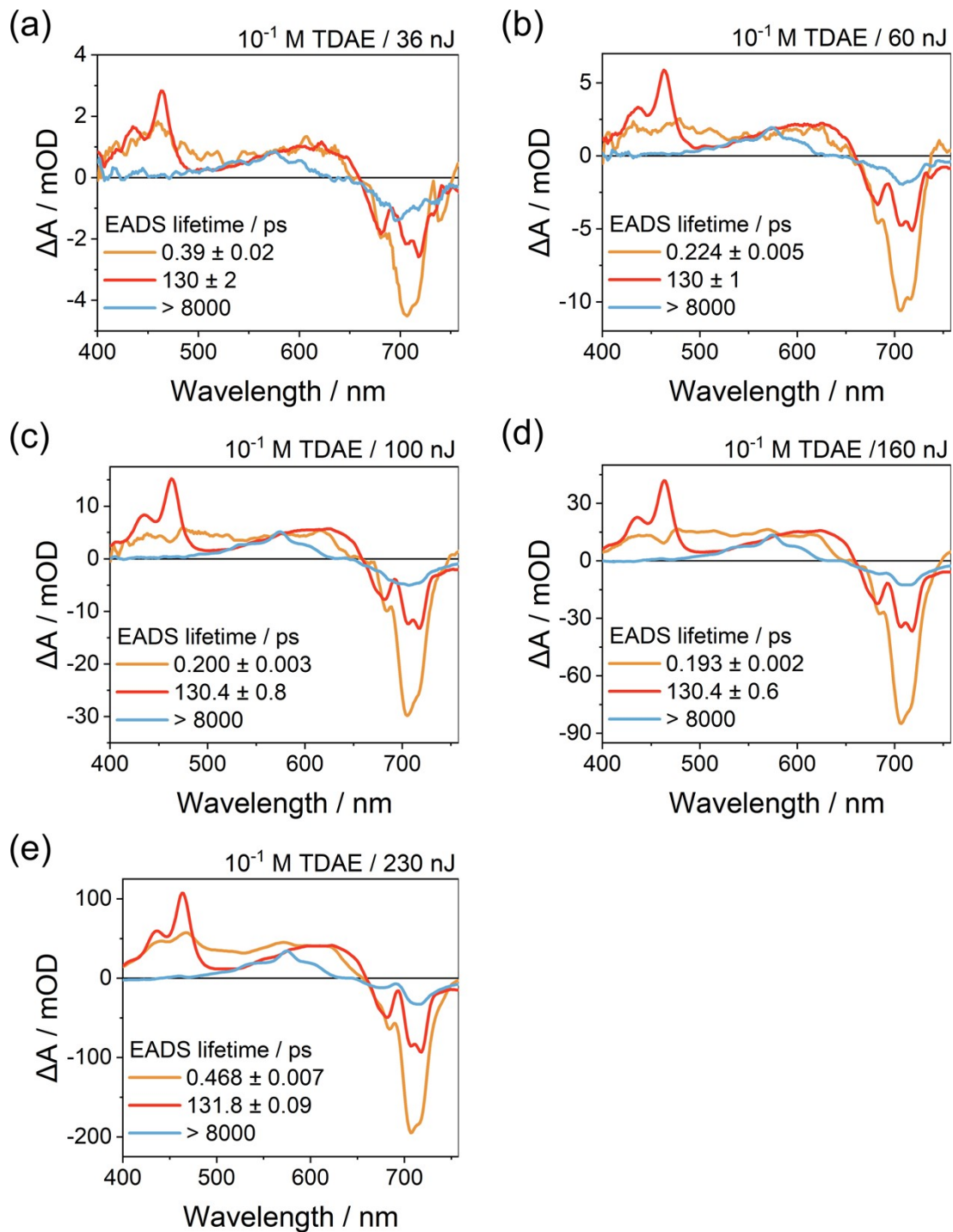
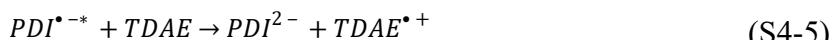
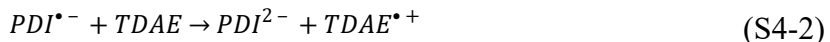


**Figure S6.** Corresponding evolution-associated difference spectra (EADS) obtained from sequential model-based global analysis under different excitation power conditions (a)36 nJ, (b)60 nJ, (c)100 nJ, (d)160 nJ, and (e)230 nJ. The retrieved time constants are indicated in the legends.

## S4. Reaction-Related Thermodynamic Calculations

The reactions that may be mentioned in the article are as follows



Given that:<sup>4, 5</sup>

$$E(TDAE / TDAE^{\bullet+}) = -0.62V \text{ vs SCE}$$

$$E(PDI^{\bullet-} / PDI) = -0.51V \text{ vs SCE}$$

$$E(PDI^{2-} / PDI^{\bullet-}) = -0.80V \text{ vs SCE}$$

$$E_{00}(PDI^{\bullet- \ast}) = 1.298eV$$

According to the Rehm-Weller equation<sup>6</sup>, the driving force of the reaction is calculated as follows:

$$\Delta G = E_{ox}(D/D^{\bullet+}) - E_{red}(A/A^{\bullet-}) \quad (S4-7)$$

$$E_{ox}(D^{\bullet-} / D^{\bullet+}) = E_{ox}(D/D^{\bullet+}) - E_{00} \quad (S4-8)$$

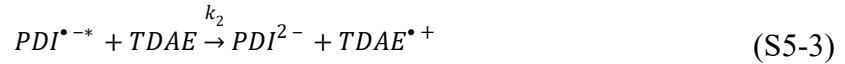
$$E_{red}(A^{\bullet-} / A^{\bullet-}) = E_{red}(A/A^{\bullet-}) - E_{00} \quad (S4-9)$$

**Table S2.** Chemical reaction equations and corresponding Gibbs free energies

reaction	$\Delta G_{ET} / \text{eV}$
$PDI + TDAE \rightarrow PDI^{\bullet-} + TDAE^{\bullet+}$	-0.11
$PDI^{\bullet-} + TDAE \rightarrow PDI^{2-} + TDAE^{\bullet+}$	0.18
$PDI^{\bullet- \ast} + TDAE \rightarrow PDI^{2-} + TDAE^{\bullet+}$	-1.118

## S5. Kinetic Simulation of Multi-Electron Transfer Reactions

The kinetics of PDI multi-electron transfer reactions were modeled based on the following reaction scheme:



Consider the generation process of  $PDI^{2-}$ , the corresponding rate equations are:

$$\frac{d[PDI^{\bullet-*}]}{dt} = -k_1[PDI^{\bullet-*}] - k_2[PDI^{\bullet-*}][TDAE] \quad (S5-5)$$

$$\frac{d[PDI^{\bullet-}]}{dt} = k_1[PDI^{\bullet-*}] \quad (S5-6)$$

$$\frac{d[PDI^{2-}]}{dt} = k_2[PDI^{\bullet-*}][TDAE] \quad (S5-7)$$

$$k = k_1 + k_2[TDAE] \quad (S5-8)$$

The system admits analytical solutions:

$$[PDI^{\bullet-*}]|_t = [PDI^{\bullet-*}]|_0 \times e^{-kt} \quad (S5-9)$$

$$[PDI^{\bullet-}]|_t = [PDI^{\bullet-}]|_0 + \frac{k_1}{k}[PDI^{\bullet-}]|_0 \times (1 - e^{-kt}) \quad (S5-10)$$

$$[PDI^{2-}]|_t = \frac{k_2[TDAE]}{k}[PDI^{\bullet-}]|_0 \times (1 - e^{-kt}) \quad (S5-11)$$

$k$  represents the total decay rate constant (total decay rate constant), indicating the overall decay rate of the excited state  $PDI^{\bullet-*}$ . The initial conditions for the simulation are known to be the same as those of the experiment. The initial concentration of PDI is 60  $\mu\text{M}$ . The lifetime of  $PDI^{\bullet-*}$  at 0.001 M TDAE is 157 ps. The simulation duration is 8 ns.

$$[PDI^{\bullet-*}]|_0 = \eta_{ex} \times [PDI]_{total} \quad (S5-12)$$

$$[PDI^{\bullet-}]|_0 = (1 - \eta_{ex}) \times [PDI]_{total} \quad (S5-13)$$

$$[PDI^{2-}]|_0 = 0 \quad (S5-14)$$

Consider the attenuation process of  $PDI^{2-}$ , the simulation duration is 5  $\mu$ s.

$$k_3 = \frac{1}{\tau_{PDI^{2-}}} \quad (S5-15)$$

The initial conditions account for different excitation efficiencies: Assuming an energy of 230 nJ, the excitation efficiency is 30%. Based on this ratio, the excitation efficiencies under different excitation powers (36 nJ, 60 nJ, 100 nJ, 160 nJ) are 4.69%, 7.83%, 13.04%, and 20.87% respectively. The lifetime of  $PDI^{2-}$  at  $10^{-1}$  M TDAE is 561 ns. Under this simulation condition, the resulting kinetic diagram is as follows:

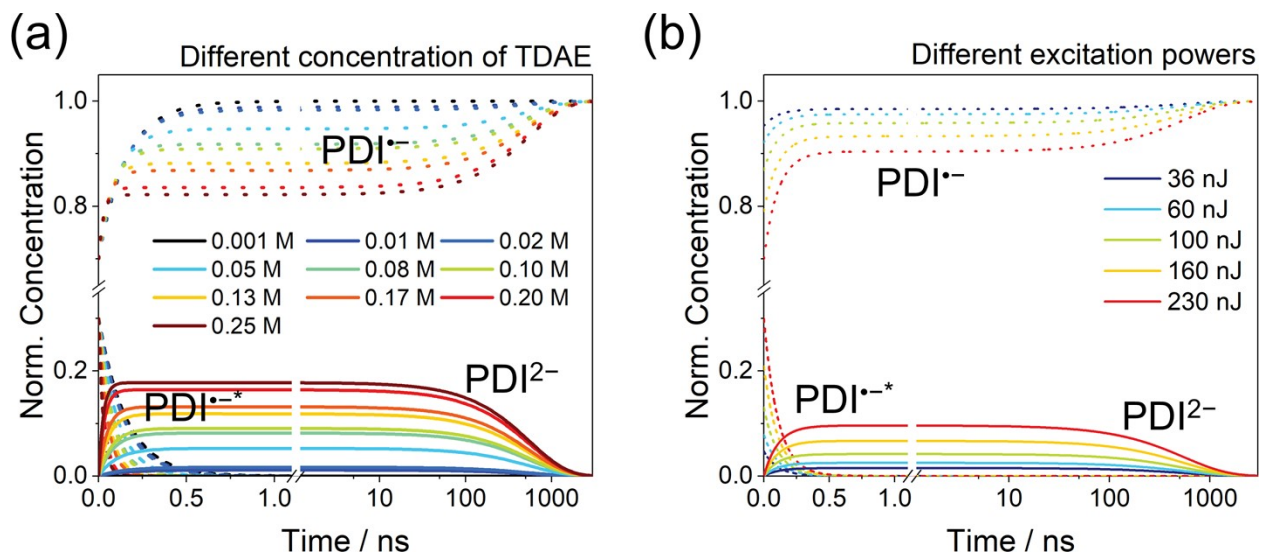


**Figure S7.** Kinetic simulation of species concentration evolution in the multi-electron transfer process under (a) different TDAE concentration and (b) different excitation powers. Species concentrations are normalized with respect to the initial  $PDI^{\bullet-}$  concentration.

## S6. Supplementary References

1. J. J. Snellenburg, S. Laptenok, R. Seger, K. M. Mullen and I. H. M. van Stokkum, *J. Stat. Soft.*, 2012, **49**, 1 - 22.
2. I. H. M. van Stokkum, D. S. Larsen and R. van Grondelle, *BBA - Bioenergetics*, 2004, **1657**, 82-104.
3. D. J. Gosztola, M. P. Niemczyk, W. A. Svec, A. S. Lukas and M. R. Wasielewski, *J. Phys. Chem. A*, 2000, **104**, 6545-6551.
4. H. Li and O. S. Wenger, *Angew. Chem. Int. Ed.*, 2022, **61**, e202110491.
5. C. Burkholder, W. R. Dolbier and M. Médebielle, *J. Org. Chem.*, 1998, **63**, 5385-5394.
6. D. Rehm and A. Weller, *Bunsen-Ges. Phys. Chem.*, 1969, **73**, 834-839.